Isolating physical effects in the exclusive $(N, N'\pi)$ reaction

R. Mehrem,* J. T. Londergan, and G. E. Walker
Department of Physics and Nuclear Theory Center, Indiana University, Bloomington, Indiana 47408
(Received 1 December 1994)

We propose a series of experimental measurements of the exclusive $(N, N'\pi)$ process on light nuclei. It is suggested that different physical effects can be isolated by the following procedures: (a) varying the incident energy of the projectile nucleon at fixed nuclear energy and momentum transfer; (b) measuring ratios of cross sections to different T_z substates of the same final nuclear isotopic mutiplet; and (c) comparing ratios of cross sections for high spin non-normal parity states to those of low spin normal parity states. We discuss each of these methods for comparing data, and show what physical information can be extracted with each method.

PACS number(s): 25.40.−h

I. INTRODUCTION

The study of intermediate energy pion production and absorption on complex nuclei remains an important element in understanding strongly interacting many-body systems. This is part of the more general topic of hadron production and propagation in the nuclear environment. In order to understand nuclear processes at high energy, or the multiplicity of particles (mainly pions) produced by very high energy colliding heavy ions, it is necessary that we understand nuclear pion production and transmission at intermediate energies. A successful study of pion production may require the use of different probes to induce the production reaction, each projectile having its characteristic advantages and limitations. The (p, π) process has historically played an important role in studying proton-induced pion production, because of the assumed elementary nature of the process and the availability of high quality data. While some progress has occurred during the past decade in understanding the theoretical aspects of the (p, π) reaction to bound or quasibound states of complex nuclei, many uncertainties remain [1–4]. Comparison of the most detailed theories with experiment has met with limited success, and it seems fair to say that the pion production reaction mechanism is not yet completely understood. One difficulty is that the (p, π) process necessarily transfers a large momentum to the nucleus ($q \sim 400$–700 MeV/c). Thus, calculations of this process are quite sensitive to "multistep" processes, theoretical input uncertainties, and details of off-shell propagators. One reason for the lack of progress in this field is the number of uncertain quantities in the (p, π) process.

Recently, we have studied the exclusive $(N, N'\pi)$ reaction to quasibound states of complex nuclei [5,6]. This reaction can be studied experimentally at existing facilities and has some theoretical advantages when compared to the (p, π) reaction. The most important advantage results from the fact that the $(N, N'\pi)$ reaction can occur at relatively low to medium nuclear momentum transfers ($q \sim 100$–300 MeV/c), as well as at the higher momentum transfers required for the (p, π) reaction.

A potential disadvantage in studying the $(N, N'\pi)$ reaction is that it requires knowledge of a large number of variables. Since this reaction involves several strongly interacting systems (the reaction involves at least three final continuum particles — the nucleon, pion, and final nuclear state), quantitative descriptions of this reaction require knowledge of initial- and final-state distorted waves, the reaction $N+N \rightarrow N+N+\pi$ in the nuclear environment, and the appropriate nuclear wave functions. In order to make some sense of this reaction, it is necessary to make a systematic study of observables which are highly sensitive to certain variables, and reasonably insensitive to others.

We have argued that it may be possible to accomplish this. Measurement of $(N, N'\pi)$ cross sections to final nuclear states of definite angular momentum, parity, and isospin allows one to use the nucleus as a "spin-isospin filter," i.e., transitions to certain final states can occur through only one, or a few, of the various reaction amplitudes. We argued that this selectivity of the exclusive $(N, N'\pi)$ reaction, together with the low nuclear momentum transfers possible, might make theoretical predictions of this process both more reliable and easier to test experimentally, than for the (p, π) reaction. These issues are discussed in detail in Ref. [5] and provide the starting points for this paper. Finally, our predicted $(N, N'\pi)$ cross sections were large enough that this process could be studied experimentally at facilities such as TRIUMF and the Indiana University Cyclotron Facility [7], although it was predicted that the maximum cross sections for this reaction would occur at somewhat higher incident proton energies [8,9].

The microscopic reaction mechanism incorporated in our earlier $(N, N'\pi)$ study [5] is the so-called two nucleon mechanism, the reaction $NN \rightarrow NN\pi$ in the nuclear medium. For the energies of interest (nucleon energies at or above 500 MeV), it is reasonable to assume

*Present address: Dept. of Physics, UAE University, P.O. Box 15551, Al-Ain, United Arab Emirates.

the process is dominated by formation of an intermediate $\Delta(1232)$. The various possible reaction amplitudes are shown schematically in Fig. 1 and all include a propagating intermediate meson and Δ. Assuming that the isobar production amplitudes dominate our cross sections, then our model requires as input the external particle distorted waves, initial- and final-bound nuclear wave functions, form factors for the baryon-meson vertices, and the self-energies of the meson and Δ.

In this paper we suggest various experimental measurements which concentrate on certain properties, and which are less sensitive to other quantities. For example,

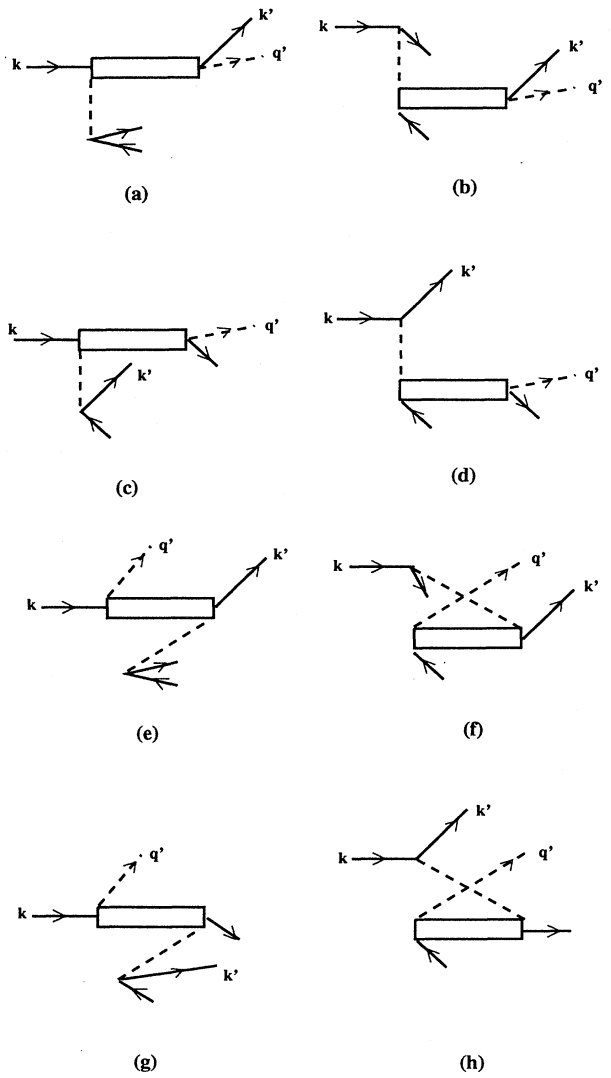

FIG. 1. Amplitudes included in the two-nucleon $(N, N'\pi)$ reaction discussed in the text. The post-emission amplitudes (a)–(d) are associated with the amplitudes $A'_1 - D'_1$, respectively, in Eq. (2), while the pre-emission amplitudes (e) - (h) are associated with the amplitudes $A'_2 - D'_2$, respectively. Mesons are represented by dashed lines. The narrow rectangle represents the intermediate Δ. Solid lines with (without) momentum labels represent continuum (bound or quasibound) nucleons.

a common technique is to take ratios of certain cross sections at the same incident proton energy, since in such ratios the absolute beam normalization cancels out. Such ratios may also be relatively insensitive to optical distortions of incident and outgoing particles. The ideas we present are similar to those already adopted in various areas of intermediate energy physics. We concentrate on three general categories.

(1) *Measurement of cross sections at different energies and angles, at fixed nuclear momentum transfer.* As the $(N, N'\pi)$ process involves three final-state particles, it is possible to arrange the experimental kinematics so the momentum transfer to the nucleus remains constant, over a range of energies (or energy loss) and detection angles for the external particles. First, this is useful because the momentum transfer to the nucleus, q_A, produces the most rapid variation in the cross section. Keeping q_A constant ensures that the reaction amplitudes vary slowly and smoothly.

In addition, several important many-body effects are strong functions of nuclear momentum transfer. We can predict the energy, scattering angle, and momentum transfer dependence of the nuclear response function. A similar idea is widely used in inelastic electron scattering, where Rosenbluth plots of the (e, e') cross section have been useful in separating longitudinal and transverse form factor contributions and testing the validity of the one photon exchange approximation [10]. Working at fixed nuclear momentum transfer and varying the projectile scattering angle has also been useful in (π, π') and (p, p') reactions, for identifying the spin and parity of excited nuclear states, studying the importance of individual terms in the transition operator, and providing tests of the distorted wave impulse approximation [11,12].

(2) *Measuring ratios of cross sections to different members of the same nuclear isotopic multiplet.* This can be useful in comparing the contribution of various reaction amplitudes for this process. For example, if a single reaction amplitude dominated all $(N, N'\pi)$ reactions, then ratios of reactions involving different final states of the same isotopic multiplet, e.g., $^{16}\mathrm{O}(p, p'\pi^+)^{16}\mathrm{N}[J^\pi = 4^-]/$ $^{16}\mathrm{O}(p, n\pi^+)^{16}\mathrm{O}[J^\pi = 4^-]$, would be simple ratios of isospin Clebsch-Gordan coefficients, and this ratio would be independent of kinematic variables such as the nuclear momentum transfer.

Strong deviation of these ratios from the isospin Clebsch-Gordan coefficients would suggest a more complicated reaction mechanism. Our calculations predict cross sections for processes leading to analog states of the same isotopic multiplet, which disagree strongly with the isospin Clebsch-Gordan coefficients. Our calculated cross-section ratios also show strong dependence on the nuclear momentum transfer (for certain charge states of the final pion-nucleon system). We will show that this ratio depends critically on the relative magnitude of "post-emission" and "pre-emission" amplitudes. "Post-emission ("pre-emission") amplitudes are those where the final-state pion is emitted when the Δ decays (is formed). For certain reactions we expect the post-emission amplitudes to dominate. In other reactions, however, we predict considerable enhancement of pre-emission ampli-

tudes relative to post-emission terms. We will show that the ratio of transitions to different states of the same isotopic multiplet (but the same J and T) depend strongly on the relative magnitude of these amplitudes.

(3) *Comparison of transitions to low-spin normal parity, and high-spin non-normal parity, nuclear states.* Previous calculations [5] have indicated that, depending on the nuclear momentum transfer, a small number of low-spin normal parity or high-spin non-normal parity final nuclear states dominate the nuclear response. This is interesting because different reaction amplitudes contribute to these dominant states. In particular, the process shown in Fig. 1(a) results only in the excitation of non-normal parity $\Delta T = 1$ states [for $(N, N'\pi)$ processes on a $T = 0$ target]. In our previous paper we showed that such transitions were especially sensitive to the nuclear medium self-energy of the virtual pion in this reaction. We showed that by taking ratios of cross sections to appropriate dominant final nuclear states, one can either exclude or accentuate the predicted effects associated with virtual meson propagation.

The comparison of ratios of cross sections in intermediate energy nuclear physics (other than to eliminate straightforward effects of external particle distortion) has a long history in nuclear physics. For example, such a procedure has been useful in comparison of (e, e'), (π, π'), and (p, p') cross sections, to eliminate nuclear structure uncertainties and study the validity of the distorted wave impulse approximation and strong interaction transition operators [13].

The outline of our paper is as follows. In Sec. II we review the basic expressions for the $(N, N'\pi)$ reaction. As these results have been outlined in considerable detail in Ref. [5], we review the results in schematic form. Our aim is to present a heuristic picture to illustrate the physics which can be extracted, when data are compiled according to the three procedures we have suggested. In Sec. III we present results obtained using the formulas given in Sec. II. The results are presented in a series of figures which are discussed at length. We also suggest future experimental studies which might be carried out with this reaction. We then summarize our results in a concluding section.

II. FORMALISM AND PROCEDURES

Our model for the differential cross sections for the $(N, N'\pi)$ reaction was discussed in detail in Ref. [5]; a complete set of equations and references can be found in that paper. In what follows we briefly summarize the main assumptions and write the cross-section expression in a schematic form sufficient for our purposes, using the notation developed in our previous paper. For completeness, in the Appendix we include a more detailed expression for one typical amplitude.

We assume that the relevant scattering amplitudes arise from the process shown schematically in Fig. 1. For these amplitudes the external pion is produced in the reaction $N + N \to N + N + \pi$ in the nuclear environment, assuming the process is dominated by Δ resonance formation. We use optical potentials to generate distortions of the external nucleons and pions. We focus on exclusive $(N, N'\pi)$ reactions leading to one-particle–one-hole states of the target nucleus. The initial (closed shell) and final (particle-hole) nuclear wave functions are described in the standard shell model as combinations of products of single nucleon orbitals [14]. Using these assumptions and the procedures discussed in Ref. [5] we may write the $(N, N'\pi)$ differential cross section in the nucleon-nucleus center-of-mass (c.m.) frame (for an initial unpolarized nucleon) as

$$\frac{d^3\sigma}{d\Omega' d\Omega_\pi dE'} = \frac{10^4}{2(2\pi)^5} \frac{k'q'E'E}{k(1 + E/E_A)} |\overline{T}_{fi}|^2, \qquad (1)$$

where $E(E')$ and $k(k')$ are the initial (final) nucleon energy and momentum, respectively. The units for the cross section in Eq. (1) are $\mu\mathrm{b/sr^2/MeV}$ (we use units where $\hbar = c = 1$). The momentum of the outgoing pion is denoted q' and E_A is the initial nuclear target energy in the c.m. frame. The amplitude $\overline{T}_{fi}$ will be the focus of our study. We will discuss sets of observables which focus on specific aspects of the transition operator, and which are less sensitive to other effects. We will attempt to separate effects in $\overline{T}_{fi}$ arising from external particle distortions, the nuclear many-body shell model wave functions, and the microscopic reaction mechanism.

We divide the scattering process into three parts: distortions of the incoming and outgoing free particles, nuclear structure effects, and a hard scattering process by which the Δ is produced and decays. We account for the distortions by using optical potentials derived from elastic scattering of medium energy nucleons [15] and pions [16]. The amplitudes contributing to the hard scattering process are shown schematically in Fig. 1. The process $N + N \to N + \Delta$ is mediated by exchange of an isovector meson (π or ρ, in our calculations). $\overline{T}_{fi}$ consists of eight amplitudes. Four of these, shown in Figs. 1(a)–1(d), are the so-called "post-emission" amplitudes, where the outgoing pion is produced when the Δ decays. The remaining four, in Figs. 1(e)–1(h), comprise the "pre-emission" amplitudes, where the outgoing pion is created when the Δ is formed.

In our original calculation we considered only the "post-emission" amplitudes, but we will show that for some reactions the "pre-emission" amplitudes should dominate. This depends primarily on the charge of the emitted pion. For certain transitions we find that some amplitudes may be dominant, while other amplitudes are negligible. There are two possible reasons for this. For exclusive transitions to certain states, spin-isospin selection rules eliminate certain terms. The nucleus acts as a "spin-isospin filter," which removes some amplitudes. In other situations, certain amplitudes may dominate for kinematic reasons. Because of the large energy transfer associated with Δ production, the various terms which contribute to the scattering amplitude correspond to virtual mesons with very different energies and momenta. In certain kinematic regions some amplitudes may be disregarded.

We may write

$$|\overline{T}_{fi}|^2 = \frac{1}{2}\sum_{s_{z_i},s_{z_f},J_z}\left|\sum_i (A_i' - B_i' - C_i' + D_i')\right|^2, \quad (2)$$

where $i = 1$ (2) refers to amplitudes associated with the postemission (pre-emission) processes shown in Fig. 1. The cross section is averaged over initial nucleon spin s_{z_i}, and summed over final nucleon spins (s_{z_f}) and nuclear angular momentum projection J_z. We can illustrate the general form of the scattering amplitude by studying the process shown in Fig. 1(a) (the detailed expression for the amplitude corresponding to Fig. 1(a) is given in the Appendix). Assuming the intermediate isovector meson is a pion, the amplitude corresponding to Fig. 1(a) can be written schematically as

$$A_1' = \frac{A_1^I F(q_A, v)}{D_\pi(q_A,\omega_A) D_\Delta(q_A^\Delta,\omega_A^\Delta)}, \quad (3)$$

where A_1^I as listed in the Appendix (see Table I) contains all the isospin dependence associated with the reaction. The term $D_\pi(q_i,\omega_i)$ is the inverse of the intermediate pion propagator and has the general form

$$D_\pi(q_i,\omega_i) = \omega_i^2 - q_i^2 - m_\pi^2 - \Pi(q_i,\omega_i), \quad (4)$$

where $\Pi(q_i,\omega_i)$ is the pion self-energy contribution. Our approximation for the self-energy includes intermediate nucleon particle-nucleon hole and Δ particle-nucleon hole ring energies calculated for an infinite medium (Fermi gas) [10,17,18], as well as a short-range repulsion characterized by a Landau-Migdal g' term. The isobar propagator term D_Δ will be given by Eq. (9). The term $F(q_A, v)$ contains the dependence of the amplitude on the momentum transferred to the nucleus, q_A, as well as all other nonisospin variables, v. This term is generally quite complicated and typical of strong interaction processes involving distortion.

The nuclear momentum transfer dependence is difficult to isolate or to characterize. However, our shell model amplitudes produce cross sections which decrease rapidly with increasing nuclear momentum transfer. For this reason it is useful to consider processes at fixed nuclear momentum transfer; in this case we expect a slow and smooth dependence of the reaction cross section on other kinematic variables. To demonstrate this, we consider the expression A_1' in the plane wave limit for a particular particle-hole transition using nuclear L-S coupling. The post-emission amplitude A_1 in plane wave approximation is given in Appendix C of Ref. [5]. We find for amplitude A_1'

$$A_1' \propto A_1^I A_1^a A_1^b, \quad (5)$$

where A_1^I is the isospin factor mentioned earlier. The other factors, which depend on geometry, coupling constants, intermediate particle propagators, and nuclear structure are given by

$$A_1^a = (-1)^{l_h} i^L \sqrt{3}\,\frac{\hat{l}_p \hat{l}_h}{\hat{J}}\,\frac{f_{\pi NN} f_{\pi N\Delta}^2}{m_\pi^3}\, C^{l_p\ l_h\ L}_{0\ 0\ 0}\, C^{L\ 1\ J}_{0\ 0\ 0}\, A^{n,n'}_{l_p,l_h,L}(q_A)\, Y^{J*}_{J_z}(\hat{\mathbf{q}}_A)\,\frac{F_A^\pi(q_A)}{D_\pi(q_A,\omega_A) D_\Delta(q_A^\Delta,\omega_A^\Delta)}, \quad (6)$$

$$A_1^b = -2\left(\frac{8\pi}{3}\right)^{\frac{3}{2}} q' q_A^2 \left[Y^1(\hat{\mathbf{q}}') \otimes Y^1(\hat{\mathbf{q}}_A)\right]^{S'}_{S_z'} \begin{Bmatrix} 1 & 1 & S' \\ \frac{1}{2} & \frac{1}{2} & \frac{3}{2} \end{Bmatrix} \delta_{S,1}, \quad (7)$$

where q_A is the nuclear momentum transfer and $A^{n,n'}_{l_p,l_h,L}(q_A)$ is the nuclear particle-hole radial matrix element which (for a given set of nuclear orbitals, nuclear size, and orbital angular momentum L) depends only on the magnitude of q_A. For the definition of other symbols in Eq. (7) see Ref. [5] and the Appendix.

The energy, ω_A (ω_A^Δ), and momentum q_A (q_A^Δ) of the intermediate pion (Δ) are related to the other energies and momenta via

$$\omega_A = E_A - E_A^\star, \qquad \mathbf{q}_A = \mathbf{k}' + \mathbf{q}' - \mathbf{k},$$
$$\omega_A^\Delta = E' + E_\pi, \qquad \mathbf{q}_A^\Delta = \mathbf{k}' + \mathbf{q}', \quad (8)$$

where $\mathbf{k}'$ ($\mathbf{q}'$) (see Fig. 1) is the momentum of the final detected nucleon (pion). For example, one can vary the

TABLE I. Values for the isospin factor A_1^I appearing in Eq. (2.3) and in the Appendix assuming a closed shell ^{16}O ground state and a final particle-hole configuration for the final nucleus and a final nuclear isospin T.

Reaction	Post-emission amplitudes				Pre-emission amplitude			
$^{16}O(N,N'\pi)$	A_1	B_2	C_1	D_1	A_2	B_2	C_3	D_4
$^{(p,n\pi^+)}_{T=1}$	$\sqrt{2}$	$\sqrt{2}$	$-\sqrt{2}/3$	$-\sqrt{2}/3$	$\sqrt{2}/3$	$\sqrt{2}/3$	$\sqrt{2}/3$	$\sqrt{2}/3$
$^{(p,n\pi^+)}_{T=1}$	$-2/3$	$-2/3$	$2/3$	$2/3$	$2/3$	$-2/3$	$2/3$	$-2/3$
$^{(p,n\pi^+)}_{T=0}$	0	0	$4/3$	$4/3$	0	$4/3$	0	$-4/3$
$^{(p,p'\pi^0)}_{T=1}$	$-2\sqrt{2}/3$	$-2\sqrt{2}/3$	0	0	$-2\sqrt{2}/3$	0	$-2\sqrt{2}/3$	0
$^{(p,p'\pi^0)}_{T=0}$	0	0	$-2\sqrt{2}/3$	$-2\sqrt{2}/3$	0	$-2\sqrt{2}/3$	0	$-2\sqrt{2}/3$
$^{(p,n\pi^0)}_{T=1}$	$2/3$	$2/3$	$-2/3$	$-2/3$	$-2/3$	$2/3$	$-2/3$	$2/3$
$^{(p,p'\pi^-)}_{T=1}$	$\sqrt{2}/3$	$\sqrt{2}/3$	$\sqrt{2}/3$	$\sqrt{2}/3$	$\sqrt{2}$	$-\sqrt{2}/3$	$\sqrt{2}$	$-\sqrt{2}/3$

kinetic energies of the incident nucleon and final detected nucleon, with the pion and nucleon angles and the energy of the pion held fixed ($\mathbf{q}'$ is thus held fixed).

In this paper we wish to focus the discussion on the predicted behavior, for fixed momentum transfer, of the various contributions to the amplitudes making up the $(N, N'\pi)$ cross section. In principle the distortion effects, which are functions of the nucleon or pion energy, can change for fixed nuclear momentum transfer. However, we are working in a kinetic energy region of approximately 50 MeV for the final pion and 100–500 MeV for the nucleons, where optical potential parameters are reasonably well known and pion absorption effects are not dramatic [16]. We compare in the next section, plane wave and distorted wave, fixed nuclear momentum transfer, and variable external nucleon energy results. Use of distorted waves could cause some changes in the energy dependence of the delta and intermediate pion propagators, because additional integrations over kinematic variables enter compared to plane wave calculations. With this caveat in mind, we now discuss the predicted external nucleon energy dependence of the intermediate delta and virtual pion propagators for fixed nuclear momentum transfer.

A. The delta propagators

Each of the eight amplitudes shown schematically in Fig. 1 has an associated Δ propagator. We assume that the general form for the inverse of the delta propagator is given by

$$D_\Delta(q^\Delta, \omega^\Delta) = \omega^\Delta - T_\Delta - M_\Delta - V_\Delta(q^\Delta, \omega^\Delta) + i\Gamma/2. \quad (9)$$

In Eq. (9) we have used $\Gamma = 115$ MeV, the free width of the Δ. We have neglected two corrections to the Δ width in the medium: Pauli modifications, which require that the nucleon produced in Δ decay have momentum greater than the nuclear Fermi momentum; and collision broadening, which increases the Δ width in the medium. Isobar-hole studies of Δ production in pion scattering calculate an increase in the Δ width in medium [19–22]. For the real Δ-nucleus interaction, we have chosen a potential whose shape follows the nuclear density and whose central value is chosen as $V_\Delta = -35$ MeV, an average nuclear potential for the Δ appropriate for the energies we are considering [19]. In Ref. [5] we estimate the effects of Pauli modifications and collision broadening on the effective width of the Δ in the nuclear medium.

In the plane wave limit and with the procedure used in Ref. [5] one can determine ω^Δ and q^Δ for each amplitude. In addition there exist symmetries between the different amplitudes of Fig. 1 that result in the following equalities:

$$D_\Delta^{A_1} = D_\Delta^{B_1}, \quad D_\Delta^{C_1} = D_\Delta^{D_1},$$
$$D_\Delta^{A_2} = D_\Delta^{C_2}, \quad D_\Delta^{B_2} = D_\Delta^{D_2}. \quad (10)$$

In Fig. 2 we plot the inverse squared Δ propagators in the center of the nucleus, as a function of the incoming nucleon kinetic energy T_p, for fixed nuclear momentum transfer. In Fig. 2(a) we plot the post-emission delta propagators $1/|D_\Delta|^2$. All have the same order of magnitude, and show a linear dependence on the nucleon kinetic energy. In Fig. 2(b) we show the pre-emission Δ propagators; the results are similar to the post-emission terms, but the magnitude of the pre-emission propagators is much smaller. The pre-emission propagators are considerably reduced because of the extra pion energy factor appearing in the energy denominator.

The propagation of isobars in nuclei has been considered in great detail in isobar-hole models of pion-nucleus interactions [19–24]. In our model we use some average local potential to estimate effects of isobar interactions in the medium. We may compare our results with those of Karaoglu and Moniz [24], who constructed a local Δ optical potential and compared the results with those

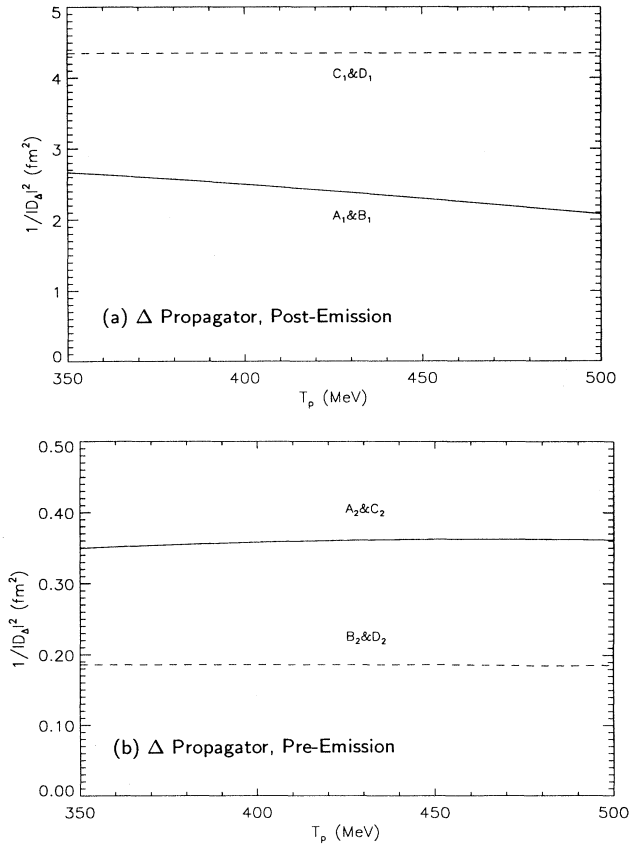

FIG. 2. (a) The variation of the square of the post-emission Δ propagators. The quantity $1/|D_\Delta|^2$ of Eq. (9) at central nuclear density, in units fm^4 is plotted vs the kinetic energy T_p of the initial nucleon. The final nucleon energy and direction is varied so the magnitude of the momentum transfer to the nucleus is fixed at 1 fm^{-1} and the nuclear excitation energy is 6 MeV. The final forward (0°) pion energy is fixed at 50 MeV. Solid curve: amplitudes A_1' and B_1' from Eq. (2); dashed curve: amplitudes C_1' and D_1'. (b) The variation of the square of the pre-emission Δ propagators. Solid curve: amplitudes A_2' and C_2' of Eq. (2); dashed curve: amplitudes B_2' and D_2'. The kinematic constraints are as in (a).

obtained from isobar-hole models. In isobar-hole models the isobar self-energy is divided into two parts, a "Pauli" term representing Pauli blocking effects whereby occupied nucleon states prohibit the process $\Delta \rightarrow \pi + N$ in the medium, and a "spreading" interaction which arises from multiparticle-hole states arising from Δ medium interactions.

The Δ-nucleus interaction is assumed to follow the nuclear density. The real part of the Δ-nucleus interaction arises from the sum of a Δ-nucleus attractive interaction, assumed to be equal to that for nucleon-nucleus scattering (with a central value $\sim$ 55 MeV), and the real parts of the Pauli and spreading potentials (both of which are repulsive and would shift the resonance energy upward). The real part of our Δ-nucleus interaction approximates the sum of these three parts. Similarly, the imaginary part of the Δ-nucleus interaction represents the combination of the Pauli term, which would produce a decrease in the Δ width by suppressing the pionic decay of a Δ in medium, and the spreading width, which would increase the Δ width (relative to its free value) due to multiparticle intermediate states reached via the $\Delta N \rightarrow NN$ interaction in medium. We have used the free Δ width in our calculations, whereas isobar-hole calculations show some overall increase in the Δ width in medium.

Finally, isobar-hole calculations find an L-dependent shift of the resonance energy in nuclei. We have not included such an effect, which tends to be repulsive for the central partial waves in pion-nucleus interactions, and attractive for the peripheral ones. Therefore our simple choice for the Δ propagator in nuclei can be expected to reproduce only some average properties of isobar propagation.

B. The intermediate pion propagators

In Fig. 3 we plot the inverse squared virtual pion propagators associated with amplitudes A and D of Fig. 1, as a function of the incident nucleon kinetic energy. The symmetry of the amplitudes leads to the following equalities:

$$D_\pi^{A_1} = D_\pi^{A_2}, \quad D_\pi^{B_1} = D_\pi^{B_2}, \quad D_\pi^{C_1} = D_\pi^{C_2}, \quad D_\pi^{D_1} = D_\pi^{D_2}. \tag{11}$$

We plot the pion propagators both with and without the pion-nuclear matter self-energy contribution, for a transition to a final nuclear state with excitation energy about 10 MeV. The results again show a smooth linear dependence of the propagators vs. the nucleon energy. The pion propagators associated with amplitudes A and D are much larger than those with amplitudes B and C. The propagators associated with amplitudes B and C carry, on average, a much larger momentum ($q_\pi \sim$ 700–800 MeV/c) than those associated with amplitudes A and D ($q_\pi \sim$ 200–300 MeV/c). The fact that the virtual pion is closer to being on shell for process A (corresponding to a pion with negligible energy and moderate momentum) results in a relatively dramatic increase in $1/|D_\pi^A|^2$ when the pion self-energy contribution is included.

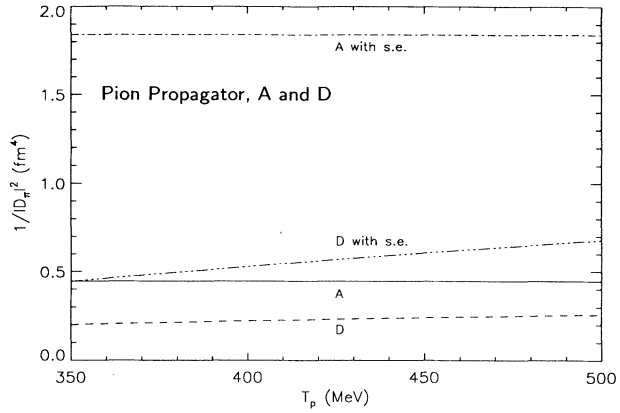

FIG. 3. The pion propagators $1/|D_\pi^A|^2$ and $1/|D_\pi^D|^2$ [corresponding to the amplitudes shown in Figs. 1(a) and 1(d), respectively] vs the incident nucleon kinetic energy T_p. The self-energy contribution contains medium modifications due to nucleon (and Δ) particle-nucleon hole rings as well as a Landau-Migdal term with $g' = 0.7$. Solid curve: pion propagator for amplitude A; dash-dotted curve: same propagator including pion self-energy contribution. Dashed curve: pion propagator for amplitude D; dash-dot-dotted curve: same propagator including pion self-energy contribution.

This is the "acoustic mode" for the pion, corresponding to very small energy ω, and moderate pion momentum q [25,26]. For pions in this kinematic region we find substantial medium effects. These appear as a significant increase in the amplitude A, which appears only for non-normal parity particle-hole transitions. Our pion self-energy calculations were carried out using a Fermi-gas approximation for the nuclear medium. It is possible that the assumption of an infinite medium overestimates the effects of the pion self-energy. In the next section we show that it should be possible to test whether large medium effects would appear in exclusive $(N, N'\pi)$ transitions to specific final nuclear states.

We believe that the preceding heuristic discussion of meson and delta propagators is useful for several reasons. First, it helps provide a qualitative understanding for the dominance of certain amplitudes. Second, angular momentum and isospin selection rules rule out some amplitudes for certain transitions. If, for example, the forbidden transitions are those with very large amplitudes, then the transition in question will be strongly suppressed. Finally, it illustrates the simple linear dependence of the propagators for fixed nucleon momentum transfer, as a function of other external kinematic variables. Thus at fixed nuclear momentum transfer, the propagators and nuclear structure terms should vary linearly as a function of nucleon energy loss in the energy regime to be studied.

III. RESULTS AND DISCUSSION

A. Results at fixed nuclear momentum transfer

In Fig. 4 we show the scattering amplitude $|\overline{T}_{fi}|^2$, for exclusive $(p, p'\pi^+)$ cross sections on a ^{16}O target,

vs the incident proton kinetic energy T_p. The quantity $|\bar{T}_{fi}|^2$ has units fm^6; the overall normalization constants are determined so that the final cross section has units μb/(sr^2 MeV), as seen from Eq. (1). We calculate transitions leading to the $J^\pi = 4^-$ nuclear state in ^{16}N; this is the "stretched" state in our one particle-one hole basis, and transitions to this state should dominate these reactions at large momentum transfer [5]. We have calculated transitions at a fixed nuclear momentum transfer $q_A = 1$ fm^{-1}. The full results are shown in Fig. 4(a), and Figs. 4(b)–4(e) show results for each amplitude separately. We have used the same proton and pion optical potentials, nuclear structure wave functions, pion-nucleon vertex functions, and other input parame-

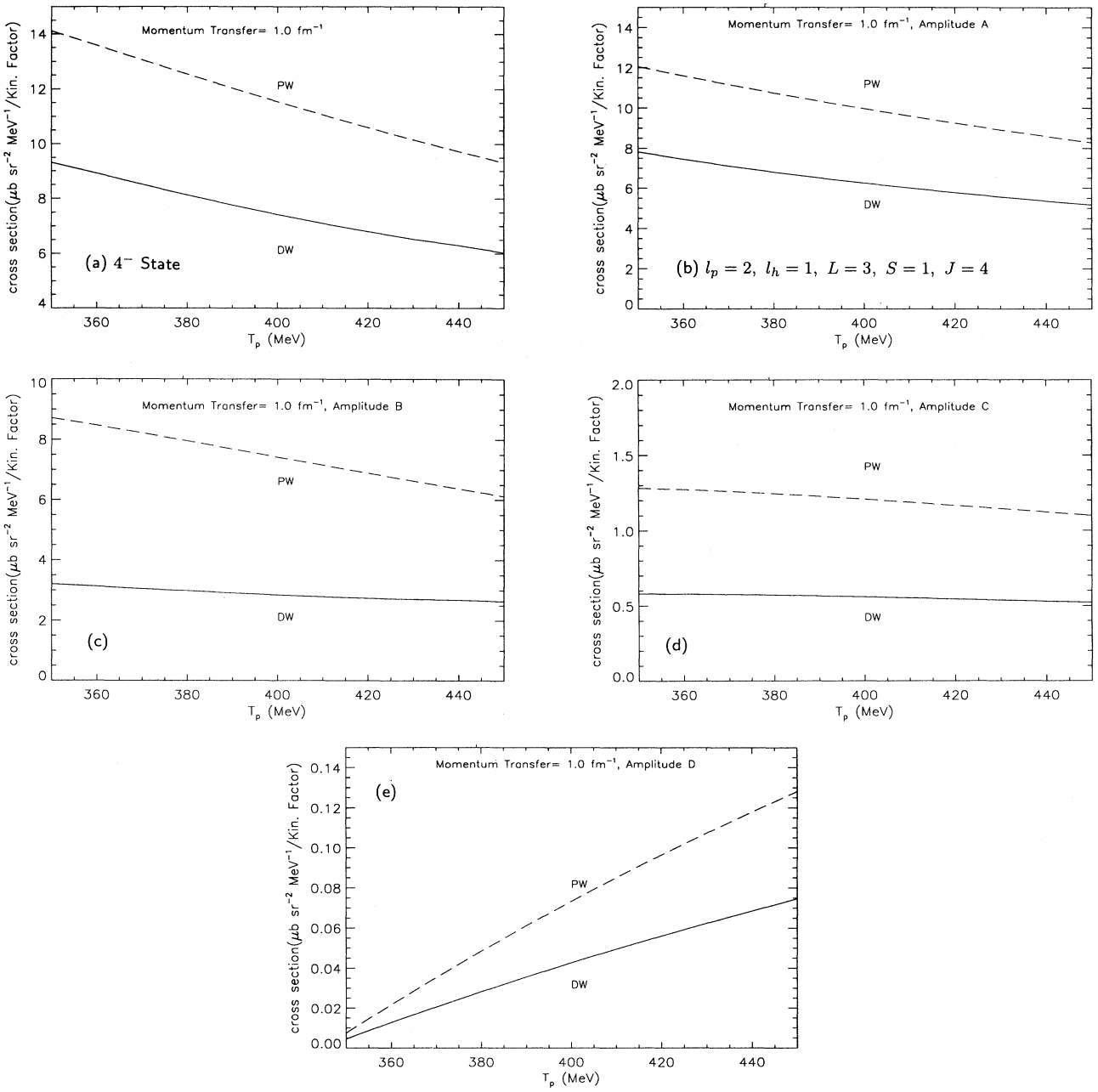

FIG. 4. (a) The scattering amplitude $|\bar{T}_{fi}|^2$ [(see Eq. (1)] for the reaction ^{16}O$(p,p'\pi^+)^{16}$N ($J^\pi = 4^-$) vs incident proton kinetic energy T_p. Solid line: distorted wave results; dashed line: plane wave results. The magnitude of the momentum transfer to the nucleus is fixed at 1 fm^{-1}. The energy of the incident proton is varied from 350 to 450 MeV. The other kinematic constraints are the same as in Fig. 2(a). This cross section includes all post-emission amplitudes given in Figs. 1(a) – 1(d). (b) Same as (a) except only the contribution of amplitude A_1 [Fig. 1(a)] is included. (c) Same as (a) except only the B_1 contribution [Fig. 1(b)] is included. (d) Same as (a) except only the C_1 contribution [Fig. 1(c)] is included. (e) Same as (a) except only the D_1 contribution [Fig. 1(d)] is included.

ters given in Ref. [5]; we have not included pion medium effects in these figures.

The results for the high spin 4^- state reveal, as expected, that both the plane wave and distorted wave results at fixed momentum transfer have a very smooth, almost linear, behavior as a function of the incident proton kinetic energy. The distorted wave results are characteristically reduced by about a factor of 2. Each of the amplitudes that contribute to this cross section also exhibits a smooth behavior when plotted at fixed momentum transfer. The largest contribution to this cross section, at this momentum transfer, is amplitude A; amplitude D makes a negligible contribution in this kinematic region, and can be ignored. All other amplitudes produce contributions which decrease smoothly with increasing proton incident energy. Furthermore, inclusion of distortions changes the magnitude, but leaves the slope of the cross sections vs proton energy essentially unchanged. Thus the rate of change of this transition, measured at constant nuclear momentum transfer, depends only rather weakly on the initial- and final-state particle distortions or nuclear wave functions. However, it does depend rather strongly on the assumed reaction mechanism, and to some extent on our assumptions regarding the range of the meson-nucleon form factors.

Consequently, measuring the variation of this transition with incident proton energy (at constant q_A) should constitute one rather strong test of the adequacy of our reaction model.

B. Cross sections leading to different charge states of the same isotopic multiplet

In Sec. II we stated that the relative importance of pre-emission and post-emission amplitudes could vary greatly for $(N, N'\pi)$ reactions leading to different final T_z states of the same isotopic multiplet. In Fig. 5, we show the contributions of post-emission and pre-emission amplitudes for the $(p, p'\pi^+)$ reaction on ^{16}O, leading to particle-hole states with $L = S = 1, J = 2$ $1d(1p)^{-1}$ character, at $E_x = 6$ MeV excitation energy for the residual nucleus ^{16}N (all subsequent results correspond to incident proton energy 450 MeV, outgoing nucleon energy 250 MeV, and scattering angle 10°). For this transition, the pre-emission contribution is completely negligible, as can be seen in Fig. 5(c), where the solid curve (both pre-emission and post-emission amplitudes included) is almost identical to the long-dashed curve, corresponding to post-emission amplitudes only. A similar conclusion can be drawn for the $(p, n\pi^+)$ reaction leading to the isobaric analog of the final nuclear state; these cross sections are shown in Fig. 6. From Fig. 6(c) we see that inclusion of the pre-emission amplitudes increases the cross section to this state by about 10%. We show plane wave results in these figures; distortions would change the absolute magnitude of the results, but none of the qualitative conclusions.

However, for the $(p, p'\pi^-)$ reaction to the isobaric analog nuclear state, the pre-emission contribution dominates, as is shown in Fig. 7. Interference effects are important for this case, as the phases and magnitudes

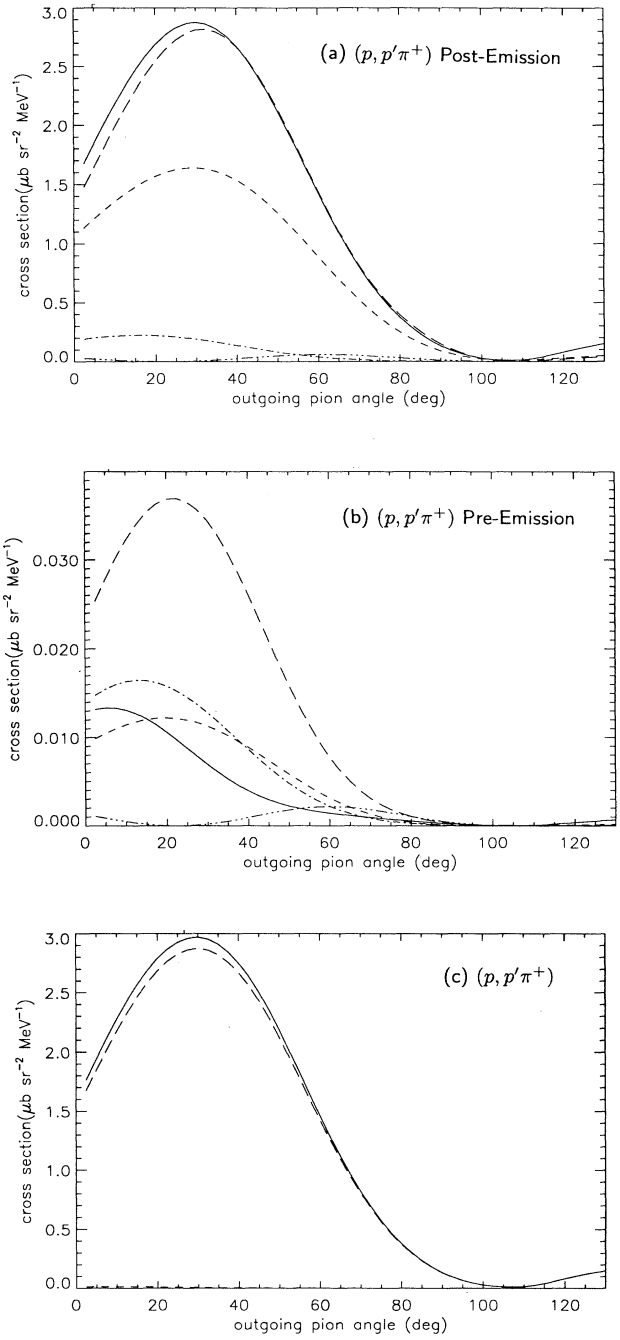

FIG. 5. (a) Plane wave results for the reaction ^{16}O$(p, p'\pi^+)^{16}$N$^*[L = S = 1, J = 2$ $1d(1p)^{-1}$ state, at $E_{ex} = 6$ MeV]. Solid curve: cross section including the four post-emission amplitudes from Figs. 1(a) – 1(d). The contribution of each individual amplitude is shown separately. Long dashed line: amplitude A_1; short dashed line: amplitude B_1; dot-dashed line: amplitude C_1; triple dot-dashed line: amplitude D_1. The incident nucleon energy is 450 MeV; the final nucleon energy is 250 MeV and angle is 10°. (b) Same as (a) except the contribution of the four pre-emission amplitudes given in Figs. 1(e)– 1(h) are shown. (c) Same as (a). Short-dashed curve: only pre-emission amplitudes included; long-dashed curve: only post-emission amplitudes included; solid curve: both post- and pre-emission amplitudes included.

(see Table I) of the individual pre-emission amplitudes interfere constructively for this transition, while the post-emission amplitudes interfere destructively. Note as mentioned earlier, the Δ propagators are substantially larger for the post-emission amplitudes for all transitions considered. Since the (relatively large) post-emission amplitudes cancel in the $(p, p'\pi^-)$ reaction, other relatively small amplitudes may contribute substantially to these transitions. For example, nonresonant amplitudes might make an important contribution to the $(p, p'\pi^-)$ reaction, and these should be included in future calculations.

In Fig. 8 we show the ratio of the cross section for the $(p, p'\pi^+)$ reaction, to those for the $(p, n\pi^+)$and $(p, p'\pi^-)$ reactions, all leading to isobaric analog states of the final nucleus. In Fig. 8(a) we show the ratios of the full cross sections; in Fig. 8(b) we show the results we would obtain using only the post-emission amplitudes. For the reactions leading to (p, π^+) and (n, π^+) final states, the

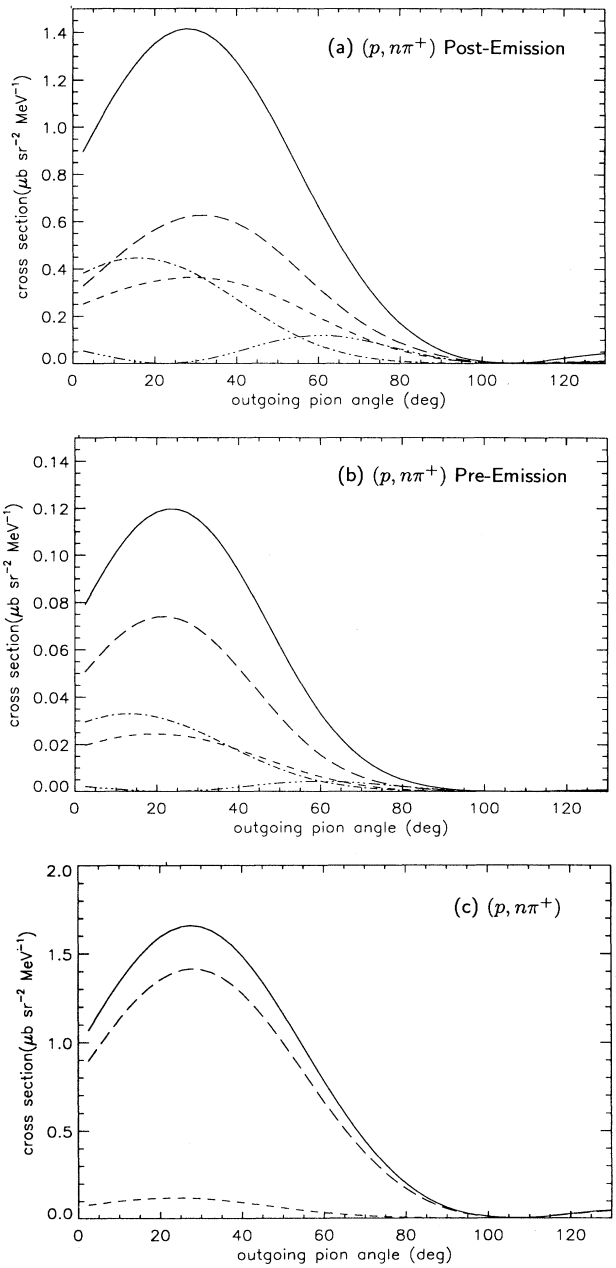

FIG. 6. (a) Same notation as Fig. 5(a), except for the $^{16}\mathrm{O}(p, n\pi^+)^{16}\mathrm{O}^*[L = S = 1, J = 2\ 1d(1p)^{-1}]$ transition. (b) Same notation as Fig. 5(b), except for the $^{16}\mathrm{O}(p, n\pi^+)^{16}\mathrm{O}^*[L = S = 1, J = 2\ 1d(1p)^{-1}]$ transition. (c) Same notation as Fig. 5(c), except for the $^{16}\mathrm{O}(p, n\pi^+)^{16}\mathrm{O}^*[L = S = 1, J = 2\ 1d(1p)^{-1}]$ transition.

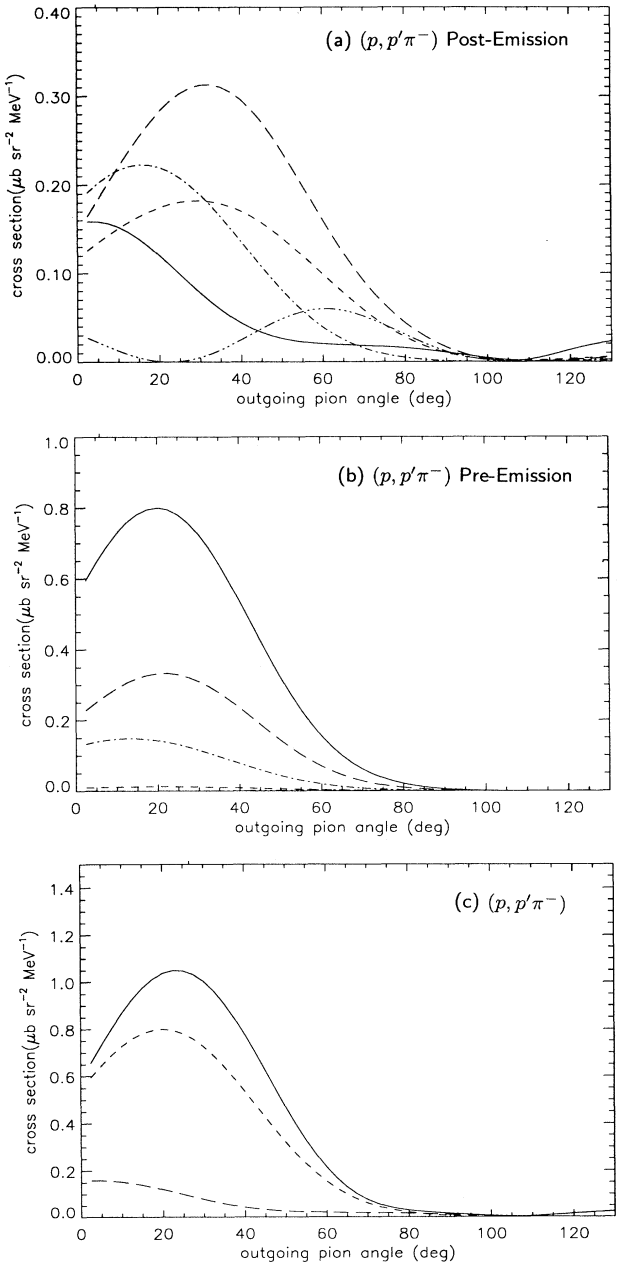

FIG. 7. (a) Same notation as Fig. 5(a) except for the $^{16}\mathrm{O}(p, p'\pi^-)^{16}\mathrm{F}^*[L = S = 1, J = 2\ 1d(1p)^{-1}]$ transition. (b) Same notation as Fig. 5(b) except for the $^{16}\mathrm{O}(p, p'\pi^-)^{16}\mathrm{F}^*[L = S = 1, J = 2\ 1d(1p)^{-1}]$ transition. (c) Same notation as Fig. 5(c) except for the $^{16}\mathrm{O}(p, p'\pi^-)^{16}\mathrm{F}^*[L = S = 1, J = 2\ 1d(1p)^{-1}]$ transition.

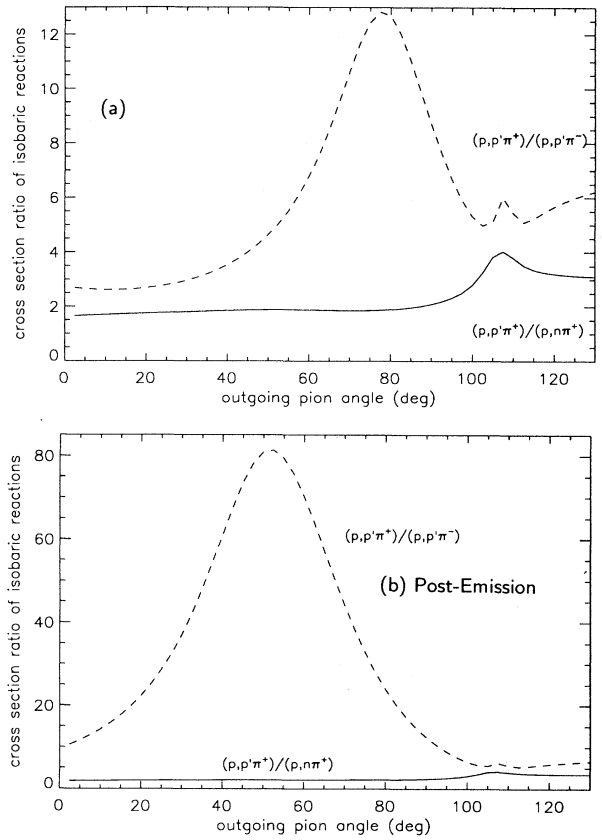

FIG. 8. (a) Ratios of the cross sections shown in Figs. 5(c), 6(c), and 7(c). Dashed curve: ratio of the cross sections for $(p,p'\pi^+)/(p,p'\pi^-)$ transitions; solid curve: ratio of cross sections for $(p,p'\pi^+)/(p,n\pi^+)$ transitions. Both pre-emission and post-emission amplitudes have been included. (b) Same as (a) except only post-emission amplitudes have been included.

cross section ratios are rather constant as a function of the outgoing pion angle, with a value between 3 and 4. Each of these cross sections is dominated by the post-emission amplitudes. The largest amplitudes for this reaction are A and B; if only these post-emission amplitudes contributed, isospin Clebsch-Gordan coefficients to these states would predict a cross section ratio of 4.5, as can be seen from Table I.

The reactions leading to (p,π^+) and (p,π^-) final states differ greatly, as the former is dominated by post-emission amplitudes and the latter by pre-emission terms. The calculated ratio has a strong dependence on outgoing pion angle, and varies between a low value of 2 and a high value of 12. If we consider only the post-emission amplitudes A and B, we would predict a ratio of 9 for these transitions, independent of scattering angle. Figure 8(a) shows these cross-section ratios including all amplitudes, and Fig. 8(b) shows the same ratios with only post-emission amplitudes included. The $(p,\pi^+)/(n,\pi^+)$ ratio is roughly the same in both figures, while the $(p,\pi^+)/(p,\pi^-)$ ratio changes dramatically when the pre-emission amplitudes are included. Thus measurement of cross sections to excite different members of the same isobaric multiplet can provide useful information about the reaction mechanism, and in particular on the importance of amplitudes other than post-emission Δ excitation.

The predicted cross sections to the isobaric nuclear states are of the same order of magnitude, so that it is plausible that all could be studied experimentally. The ratios should be relatively independent of details of the distortions, and meson self-energies. The predicted ratios depend strongly on our assumptions about the hard scattering amplitudes shown in Fig. 1. Comparing the ratios of these transitions would test directly the hard scattering assumptions in our model.

C. Ratios of cross sections for dominant transitions with different spin and parity

As discussed earlier the spin and isospin selection rules operate selectively for different amplitudes. Thus for a nuclear final state with a given spin-isospin character, certain amplitudes may dominate, or they may be forbidden to contribute to that state. Thus by observing certain transitions we can obtain information on specific scattering amplitudes; for this reason we say that the nucleus serves as a "spin-isospin filter" for Δ formation amplitudes. Because of the number of amplitudes which contribute to such processes, this property is extremely useful in sorting out the various reaction amplitudes.

In Ref. [5] we pointed out a case where this selectivity can be used to determine information about the reaction. Because of the large energy transfer needed to produce the Δ resonance, the various amplitudes shown in Fig. 1 correspond to very different kinematics (energy-momentum transfer) for the virtual isovector meson which mediates Δ formation. As a result, we predicted that the various amplitudes would be affected quite differently by medium effects (self-energies) of the virtual mesons. The pion medium corrections were particularly important for amplitude A [shown in Fig. 1(a)] because (for low-energy nuclear excitations) this amplitude corresponded to virtual mesons with small energies and moderate three-momenta.

For pions in this kinematic region, the pion propagator denominator is rather large (the pion is close to being on-shell). Thus, relatively modest changes due to medium effects can result in appreciable changes in the predicted cross section. As a specific example we consider the $(p,p'\pi^+)$ reaction leading to the $J^\pi = 4^-, T = 1$ state in ^{16}N, and to the $J^\pi = 1^-, T = 1$ "giant resonance" state. We show the 4^- cross sections in Fig. 9, and the 1^- cross sections in Fig. 10. Each transition should be dominated by contributions from one or two amplitudes (amplitude A for the 4^- state, and B and D for the 1^- transition).

We choose these states because they should be among the very largest observed transitions. The 1^- giant resonance state is a normal-parity transition, and should peak at rather low nuclear momentum transfer $q_A \sim 1$ fm^{-1}. The 4^- state is a non-normal parity transition

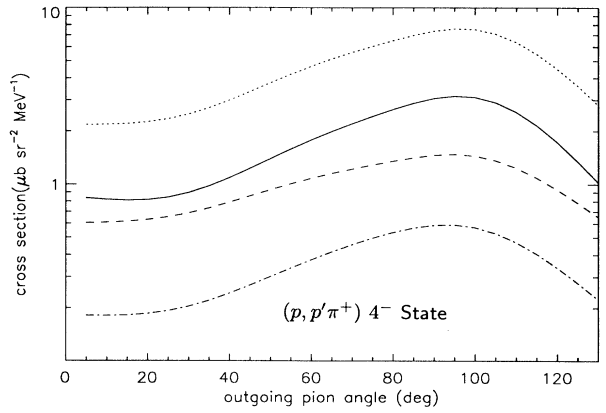

FIG. 9. Cross sections for the $^{16}O(p,p'\pi^+)^{16}N^*(4^-,T=1)$ reaction as a function of outgoing pion angle. The incident nucleon kinetic energy is 450 MeV; the outgoing nucleon kinetic energy is 250 MeV, and scattering angle is 10°. Dotted curve: plane wave calculation including pion medium effects; dashed curve: plane wave calculation neglecting medium effects; solid curve: distorted wave calculation including medium effects; dash-dotted curve: distorted wave calculation neglecting medium effects.

which should peak at substantially larger momentum transfer. This is apparent from Figs. 9 and 10, as the nuclear momentum transfer increases with the outgoing pion angle. The 1^- transition peaks at much smaller pion angle than does the 4^- reaction. Since amplitude A contributes only to non-normal parity transitions for this reaction, it makes no contribution to 1^- excitation. Therefore, the large self-energy enhancements seen for this amplitude will contribute to the 4^- cross sections but not to the 1^- state, and this can be seen in Figs. 9 and 10.

This can also be seen in Fig. 11, where we plot the ratio of cross sections calculated for the 4^- and 1^- states, with and without the self-energy contribution from the virtual pion state. We see that the self-energies are predicted to make a considerable enhancement in this ratio. This ratio is relatively independent of distortion effects and nuclear

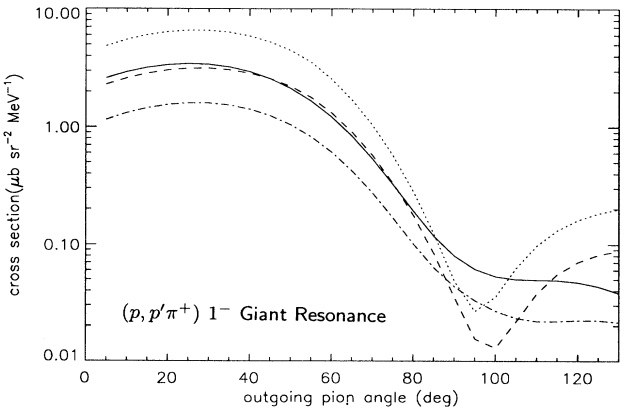

FIG. 10. Same as Fig. 9 except for the $^{16}O(p,p'\pi^+)^{16}N^*(1^-,T=1)$ giant resonance transition.

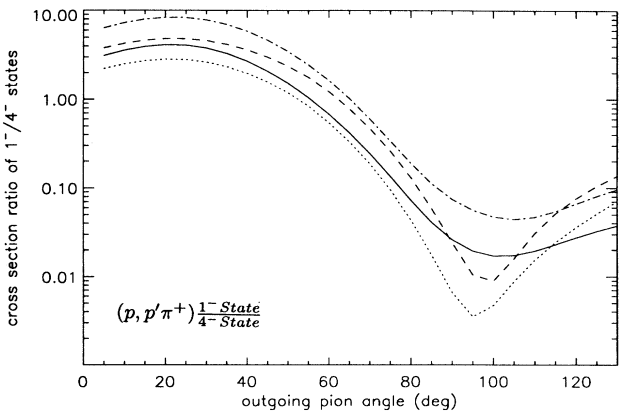

FIG. 11. The ratio of the cross sections shown in Figs. 9 and 10. The ratio $\frac{d\sigma}{d\Omega}(0^+ \rightarrow 1^-)/\frac{d\sigma}{d\Omega}(0^+ \rightarrow 4^-)$ is shown. Curves are as described in Fig. 9.

structure. In estimating medium effects for mesons in light nuclei we used a Fermi-gas model for the nuclear medium. It is possible that this assumption causes us to overestimate the pion self-energy, since the Fermi-gas model assumes an infinite medium. If so, measurement of ratios of cross sections to the 1^- and 4^- states, in the $(p,p'\pi^+)$ reaction on ^{16}O, should answer this question.

Although observation of individual transitions give us useful information on this reaction, measurement of ratios of transitions allows us to remove the dependence on a few reaction variables; for a reaction which depends on so many quantities this is an extremely valuable property.

IV. CONCLUSIONS

In a previous paper we had presented a two-nucleon model for the exclusive $(N,N'\pi)$ reaction, in a region dominated by Δ isobar formation. As this model depends on a number of assumptions regarding particle form factors, medium effects on intermediate mesons and isobars, and distortions of several continuum particles, in this paper we have examined the dependence of our results on several of these quantities. We have attempted to find observables, or combinations of observables, which are rather sensitive to certain of these parameters, and much less sensitive to others.

First, we showed that comparisons of cross sections at fixed momentum transfer to the nucleus (but different outgoing energies and/or angles) should exhibit a smooth, slow, and characteristic dependence on the incident nucleon kinetic energy. This behavior depends primarily on the form we assume for the elementary $NN \rightarrow NN\pi$ interaction in the nuclear medium. Deviation of the cross sections (at fixed nuclear momentum transfer) from this smooth behavior would suggest that the elementary interaction does not follow our assumed form.

Next, we discussed the information which can be obtained by measuring proton-induced pion production in the $(N,N'\pi)$ reaction, and comparing cross sections leading to different pion charge states. In particular, our

calculations suggest that the $(p,p'\pi^+)$ and $(p,p'\pi^-)$ reactions (leading to analog states of the final nucleus) proceed quite differently. In the $(p,p'\pi^+)$ reaction on ^{16}O, the dominant amplitudes are the "post-emission" terms, where the pion is emitted following the decay of the Δ. In the $(p,p'\pi^-)$ reaction, however, we predict very large cancellations between different post-emission amplitudes, so that the most important amplitudes for this process are the pre-emission amplitudes where the pion is emitted when the Δ is formed. We show how measurements of these cross sections would test this hypothesis.

Δ production in the nucleus occurs when a virtual isovector meson interacts with the incident proton. For virtual pions we predict substantial medium effects for certain amplitudes. We discuss how the nucleus can be used as a "spin-isospin filter" for this process, since (for a spin-0, isospin-0 target) only $\Delta S = \Delta T = 1$ (non-normal parity, $T = 1$) states are excited by this amplitude. Therefore, comparing excitation of normal-parity states to non-normal parity states in the final nucleus, should show a substantial enhancement of the non-normal parity states. We demonstrate this for the excitation of $J^\pi = 4^-$ and 1^- states for the $(p,p'\pi)$ reaction on ^{16}O.

In summary, we have presented examples of techniques for isolating the physical effects associated with intermediate meson propagation, inclusion of pre- and post-emission amplitudes, and the gross kinematic dependencies of the assumed reaction mechanism. Experimental results that allow application of these techniques would be useful in studying the appropriateness of the assumed mechanism for interpreting $(N,N'\pi)$ experiments.

ACKNOWLEDGMENTS

The authors would like to thank B.K. Jain and S. Yen for stimulating discussions regarding this problem. One author (R.M.) wishes to thank Lawrence Livermore Laboratory for its support during the writing of this paper. This research was supported in part by the U.S. NSF under Contract No. NSF-PHY91-08036.

APPENDIX

In this appendix we summarize the expression for one of the amplitudes [A_1, see Fig. 1(a)] contributing to the $(N,N'\pi)$ process. More discussion and details of the derivation are available in Ref. [5]. We assume an effective nonrelativistic Lagrangian with coupling constants and vertex functions, as given in Eq. (2.3) of Ref. [5]. Distorted waves are obtained from optical potentials for nucleons and pions in this energy region [15,16]. The incoming spin-averaged nuclear distorted wave has the form

$$\chi^+(\mathbf{k},\mathbf{r}) = 4\pi \sum_{\ell_1 m_1} (i)^{\ell_1} Y^{\ell_1}_{m_1}{}^*(\hat{\mathbf{k}}) Y^{\ell_1}_{m_1}(\hat{\mathbf{r}}) \psi_{\ell_1}(k,r) \ . \quad \text{(A1)}$$

The outgoing pion distorted wave is written

$$\chi^{(-)}_\pi(\mathbf{k},\mathbf{r}) = 4\pi \sum_{\ell_3 m_3} (-i)^{\ell_3} Y^{\ell_3}_{m_3}(\hat{\mathbf{k}}) Y^{\ell_3}_{m_3}{}^*(\hat{\mathbf{r}}) \xi_{\ell_3}(k,r) \ . \quad \text{(A2)}$$

The initial target nucleus is assumed to be a closed shell. The final nuclear excited states are assumed to be a linear combination of particle-hole states. Harmonic oscillator orbitals $\Phi^n_{l_p\, l_{z_p}}(\mathbf{r})$ $\left[\Phi^{n'}_{l_h l_{z_h}}(\mathbf{r})\right]$ are used for single bound nucleon particle (hole) states.

For process A_1 the projectile nucleon (asymptotic momentum $\mathbf{k}$) is excited to a Δ isobar through meson exchange with a target nucleon. The isobar subsequently decays into a final continuum nucleon ($\mathbf{k}'$) and pion ($\mathbf{q}'$). The initial closed shell target is excited to a nuclear particle-hole state by interaction with the incident continuum nucleon. The expression for the amplitude A_1 is given by

$$\begin{aligned} A_1 = A_1^I \frac{f_{\pi NN} f^2_{\pi N\Delta}}{m^3_\pi} & \sum_{s_{z_p}, s_{z_h}} \sum_{m_p, m_h} \sum_{L_z, S_z} (-1)^{\frac{1}{2} - s_{z_h} + l_h - m_h} C \begin{matrix} \frac{1}{2} & \frac{1}{2} & S \\ s_{z_p} & -s_{z_h} & S_z \end{matrix} \\ & \times C \begin{matrix} l_p & l_h & L \\ l_{z_p} & -m_h & L_z \end{matrix} C \begin{matrix} L & S & J \\ L_z & S_z & J_z \end{matrix} \int \frac{d^3q}{(2\pi)^3} \int d^3r_1 \int d^3r_2 \\ & \times (4\pi)^3 \sum_{l_1, m_1} \sum_{l_2, m_2} \sum_{l_3, m_3} (i)^{l_1 - l_2 - l_3} Y^{l_1}_{m_1}(\hat{\mathbf{k}}) Y^{l_2}_{m_2}(\hat{\mathbf{k}}') Y^{l_3}_{m_3}(\hat{\mathbf{q}}') Y^{l_1 *}_{m_1}(\hat{\mathbf{r}}_1) Y^{l_2 *}_{m_2}(\hat{\mathbf{r}}_1) \\ & \times \psi_{l_1}(k,r_1) \psi_{l_2}(k',r_1) \frac{\exp[i\mathbf{q}\cdot(\mathbf{r_1}-\mathbf{r_2})]}{D_\pi(q,\omega_A) D_\Delta(q^\Delta_A, \omega^\Delta_A)} \Phi^{n*}_{l_p, m_p}(\mathbf{r}_2) \Phi^{n'}_{l_h, m_h}(\mathbf{r}_2) \\ & \times \langle s_p | \sigma \cdot \mathbf{q} | s_h \rangle \langle s_f | \left[Y^{l_3 *}_{m_3}(\hat{\mathbf{r}}_1) \xi_{l_3}(q', r_1) \right] (\mathbf{S} \cdot \overleftarrow{\nabla}) (\mathbf{S}^\dagger \cdot \mathbf{q}) | s_i \rangle . \end{aligned} \quad \text{(A3)}$$

This is Eq. (2.24) of Ref. [5]. The symbol $C \begin{matrix} l_1 & l_2 & l_3 \\ m_1 & m_2 & m_3 \end{matrix}$ denotes the usual Clebsch-Gordan coefficient, and $\sigma[S]$ is a Pauli [2×4 transition] spin operator. The isospin dependent term A^I is given by

$$A^I_1 = \sum_{t_{z_p}, t_{z_h}} (-1)^{1/2 - t_{z_h}} C^{1/2\ 1/2\ T}_{t_{z_p}\ -t_{z_h}\ T_z} \langle t_p | \tau \cdot \hat{\phi}^\dagger | t_h \rangle \langle t_f | (T)_{-\lambda'} (\hat{\phi}'_{-\lambda'})^\dagger (\mathbf{T}^\dagger \cdot \hat{\phi}) | t_i \rangle \ . \quad \text{(A4)}$$

The virtual (outgoing final) pion unit vector field is denoted $\hat{\phi}$ ($\hat{\phi}'$) in Eq. (A4). The isospin (and Z projection) of the final nuclear excited state is denoted T (T_z) and λ' is the spherical index for the final outgoing pion isospin projection. The isospin dependent terms are listed for various processes in Table I. For example, A_1^I is given from Table I as $\sqrt{2}\delta_{T,1}$. Standard angular momentum coupling techniques [27] are used to reduce this expression to a calculable form in Ref. [5].

[1] *Proceedings of the Conference on Pion Production and Absorption in Nuclei*, edited by R. D. Bent, AIP Conf. Proc. No. 79 (AIP, New York, 1982).

[2] B. Hoistad, Adv. Nucl. Phys. **11**, 135 (1979); D.F. Measday and G.A. Miller, Annu. Rev. Nucl. Part. Sci. **29**, 121 (1979); H.W. Fearing, Prog. Part. Nucl. Phys. **7**, 113 (1981); G.E. Walker, Comments Nucl. Part. Phys. **A11**, 169 (1983); D.A. Ashery and J.P. Schiffer, Annu. Rev. Part. Sci. **36**, 207 (1986).

[3] H.S. Sherif, S.W. Leung, A.W. Thomas, and G. Brookfield, Phys. Lett. **83B**, 293 (1979).

[4] W.W. Jacobs *et al.*, Phys. Rev. Lett. **49**, 855 (1982); S.E. Vigdor *et al.*, *ibid.* **49**, 1314 (1982); Z-J. Cao, R.D. Bent, H.A. Nann, and T.E. Ward, Phys. Rev. C **35**, 625 (1987); T.G. Throwe *et al.*, *ibid.* **35**, 1083 (1987); E. Korkmaz *et al.*, Phys. Rev. Lett. **58**, 104 (1987).

[5] R. Mehrem, J.T. Londergan, and G.E. Walker, Phys. Rev. C **48**, 1192 (1993).

[6] Rami Mehrem, Ph.D. thesis, Indiana University, 1992, (unpublished).

[7] S. Yen, private communication.

[8] B.K. Jain, J.T. Londergan, and G.E. Walker, Phys. Rev. C **37**, 1564 (1988).

[9] B.K. Jain, N.L. Kelkar, and J.T. Londergan, Phys. Rev. C **43**, 271 (1991); **47**, 1701 (1993).

[10] T. deForest, Jr. and J.D. Walecka, Adv. Phys. **15**, 1 (1966).

[11] E.R. Siciliano and G.E. Walker, Phys. Rev. C **23**, 2661 (1981).

[12] G.E. Walker and T.N. Taddeucci, Phys. Rev. C **27**, 2777 (1981).

[13] F. Petrovich, W.G. Love, A. Picklesimer, G.E. Walker, and E.R. Siciliano, Phys. Lett. **95B**, 166 (1980).

[14] T. W. Donnelly and G.E. Walker, Ann. Phys. (N.Y.) **60**, 209 (1970).

[15] H-O. Meyer, J.R. Hall, W.W. Jacobs, P. Schwandt, and P.P. Singh, Phys. Rev. C **24**, 1734 (1981); R. Bent, private communication.

[16] K. Stricker, H. McManus, and J.A. Carr, Phys. Rev. C **19**, 929 (1979).

[17] E. Oset and A. Palanques-Mestre, Nucl. Phys. **A359**, 289 (1981).

[18] V.F. Dmitriev and T. Suzuki, Nucl. Phys. **A438**, 697 (1985).

[19] M. Hirata, J.H. Koch, F. Lenz, and E.J. Moniz, Phys. Lett. **70B**, 281 (1977); M. Hirata, F. Lenz, and K. Yazaki, Ann. Phys. (N.Y.) **108**, 116 (1977); M. Hirata, J.H. Koch, F. Lenz, and E.J. Moniz, *ibid.* **120**, 205 (1979); J.H. Koch and E.J. Moniz, Phys. Rev. C **20**, 235 (1979).

[20] L.S. Kisslinger and W.L. Wang, Phys. Rev. Lett. **30**, 1071 (1973); Ann. Phys. (N.Y.) **99**, 374 (1976).

[21] W. Weise, Nucl. Phys. **A278**, 402 (1977); E. Oset and W. Weise, Phys. Lett. **77B**, 159 (1978); Nucl. Phys. **A319**, 477 (1979); **A322**, 365 (1979).

[22] Y. Horikawa, M. Thies, and F. Lenz, Nucl. Phys. **A345**, 386 (1980); F. Lenz, E.J. Moniz, and K. Yazaki, Ann. Phys. (N.Y.) **129**, 84 (1980); F. Lenz, M. Thies, and Y. Horikawa, *ibid.* **140**, 266 (1982); M. Thies, Nucl. Phys. **A382**, 434 (1982).

[23] Z. Grossman, F. Lenz, and M.P. Locher, Ann. Phys. (N.Y.) **84**, 348 (1974).

[24] B. Karaoglu and E.J. Moniz, Phys. Rev. C **33**, 974 (1986).

[25] G.E. Brown and W. Weise, Phys. Rep. **27**, 1 (1976).

[26] E. Oset, H. Toki, and W. Weise, Phys. Rep. **83**, 282 (1982).

[27] A. deShalit and I. Talmi, *Nuclear Shell Theory* (Academic, New York, 1963).